Quantitative Measures of Coronary Stenosis Severity by 64-Slice CT Angiography and Relation to Physiologic Significance of Perfusion in Nonobese Patients: Comparison with Stress Myocardial Perfusion Imaging

Akira Sato[1], Michiaki Hiroe[2], Mieko Tamura[1], Hirokazu Ohigashi[1], Toshihiro Nozato[1], Hiroyuki Hikita[1], Atsushi Takahashi[1], Kazutaka Aonuma[3], and Mitsuaki Isobe[4]

[1]Department of Cardiology, Yokosuka Kyosai Hospital, Yokosuka, Japan; [2]Department of Nephrology and Cardiology, International Medical Center of Japan, Tokyo, Japan; [3]Department of Cardiology, University of Tsukuba Graduate School of Comprehensive Human Science, Tsukuba, Japan; and [4]Department of Cardiovascular Medicine, Tokyo Medical and Dental Postgraduate School of Medicine, Tokyo, Japan

Coronary stenosis severity by 64-slice CT angiography (CTA) is acceptably correlated with intravascular ultrasound. Stress myocardial perfusion imaging using SPECT is an established method for assessment of the functional significance of coronary stenosis. Our aim was to assess a clinical validation of quantitative measurements of coronary stenosis severity by 64-slice CTA and the relation to the physiologic significance of myocardial perfusion. **Methods:** One hundred four patients with suspected coronary artery disease underwent 64-slice CTA and stress ^{201}Tl SPECT. The stenosis severities of 105 coronary lesions assessed by CTA with sufficient image quality were compared with the results of stress ^{201}Tl SPECT. The body mass index (BMI) of the patients was 23.8 kg/m^2 (range, 21.1–25.6 kg/m^2). **Results:** Reversible defects began to increase progressively when the area of stenosis was at least 60%, and the prevalence of these reversible defects and their severity significantly increased as the degree of stenosis increased. When stenosis severity by CTA is $<$ 60%, ischemia is seldom observed; when stenosis severity is $\geq$80%, ischemia is common (86%). For intermediate stenosis severity values of 60%–70%, the prevalence of reversible defects was 9 of 27 vessels (33%), and for stenosis severity values of 70%–80%, the prevalence was 20 of 37 vessels (54%). When evaluating the diagnostic accuracy of stenosis severity by CTA to identify patients with ischemia excluding all nonevaluable vessels, applying stenosis thresholds of $>$70% results in 79% sensitivity, 92% specificity, 66% positive predictive value, and 96% negative predictive value. A lesion minimal luminal cross-sectional area of $<$ 3.7 mm^2 was a good accurate cutoff value for significant coronary narrowing using stress SPECT, with a sensitivity of 88% and specificity of 83% by receiver-operating-characteristic analysis. **Conclusion:** Despite an excellent negative predictive value to rule out the presence of ischemia, 64-slice CTA alone is a poor discriminator of the functional significance of myocardial ischemia in a highly selected patient population with a low BMI.

Key Words: CT angiography; imaging; ultrasound; coronary stenosis; perfusion

J Nucl Med 2008; 49:564–572
DOI: 10.2967/jnumed.107.042481

Over the past decade, coronary angiography has been used as the gold standard for the diagnosis of coronary narrowing and clinical decision making for coronary interventions. However, coronary angiography has several limitations, including the substantial interpretation variability of visual estimates and assessment of lesion severity for diffuse atherosclerotic lesions and intermediate-severity lesions (*1–3*).

Stress myocardial perfusion imaging (MPI) using SPECT is an established method for assessment of the functional significance of coronary stenosis and delivers valuable information for risk stratifications. Patients with stable angina and normal MPI findings have a low risk for cardiac events; therefore, no coronary intervention may not be required for these patients (*4–6*). Quantitative intravascular ultrasound (IVUS) indices can be reliably used for identifying significant epicardial coronary stenosis (*7*). Myocardial fractional flow reserve appears to be a useful index of the functional stenosis severity in patients with moderate-severity coronary stenosis (*8*). However, these modalities are invasive and relatively expensive procedures that should be avoided in low- or moderate- risk patients with a good natural prognosis.

Received Apr. 4, 2007; revision accepted Dec. 6, 2007.
For correspondence or reprints contact: Akira Sato, MD, Department of Cardiology, Yokosuka Kyosai Hospital, 1-16 Yonegahamadori, Yokosuka, Kanagawa 238-8558, Japan.
E-mail: asato@yf6.so-net.ne.jp

The recent advent of multidetector CT angiography (CTA) has greatly improved the image quality and, therefore, may allow more precise evaluation of coronary stenosis (*9–11*). Plaque and lumen area measurements derived by 64-slice CTA have also been reported to show good correlations with IVUS (*12*). The aim of the present study was to provide an early validation of quantitative measurements of coronary stenosis severity by 64-slice CTA and the relation to physiologic significance of myocardial perfusion, in comparison with stress ^{201}Tl SPECT.

MATERIALS AND METHODS

Study Population

We studied 104 consecutive patients with suspected coronary artery disease (CAD) who underwent 64-slice CTA and stress ^{201}Tl SPECT from June 2005 to December 2005 and fulfilled the following criteria: sinus heart rhythm; no previous myocardial infarction, no previous percutaneous coronary intervention or coronary bypass surgery, no unstable angina, and stable angina without 3-vessel disease. The pretest likelihood of CAD was determined according to the Diamond and Forrester method using percentage cutoffs of $<$13.4%, $>$87.2%, and in-between for low, high, and intermediate pretest likelihood, respectively (*13*). Written informed consent was obtained from all patients and the study protocol was approved by our institutional review board.

64-Slice CTA Scanning Procedure

Scanning was performed using a 64-slice CT scanner (Aquilion 64; Toshiba Medical Systems Corp.). The Aquilion 64 is a 64 × 0.5 mm collimation scanner with a gantry rotation speed of 400 ms per rotation. Scanning was performed at 120 kV and 400 mA·s, and the table feed was 6.4 mm per gantry rotation with a beam pitch of 0.2. The CT dose index volume and dose·length product of this scan protocol were 75.2 mGy and 1.10 Gy·cm, respectively. Reconstruction was routinely performed using a window centered at 75% of the R–R interval to coincide with left ventricular diastasis. A volume of 60 mL of contrast agent (Iopamidol 370, 370 mgI/mL; Schering AG) was injected intravenously at a rate of 4 mL/s. As soon as the signal density level in the ascending aorta reached a predefined threshold of 100 Hounsfield units (HU), acquisition of CT data and an electrocardiogram (ECG) trace were automatically started during a 7- to 9-s breath-hold. The patients were given oral metoprolol (20–40 mg) at 1 h before the scheduled scan if their heart rate was $>$70 beats/min, and all patients were given sublingual nitroglycerin (0.3 mg) 5 min before the scan.

Reconstruction and Image Analysis of CTA

Analysis of the scans was performed using a ZIOSTATION workstation (ZIOSOFT Inc.). Images were initially reconstructed at 75% of the cardiac cycle with a slice thickness of 0.5 mm at an increment of 0.3 mm. Spatial resolution is 0.33 mm. In case of motion artifacts, additional reconstructions were made in different time points of the R–R interval. Each scan was analyzed independently by 2 experienced readers who were unaware of the results of the IVUS and stress ^{201}Tl SPECT.

The image display settings for the lumen and plaque quantification were determined according to previously published data (*12*). In the first step, 32 coronary sites in 8 patients (4 different coronary sites in each patient) with stable angina pectoris who previously underwent 64-slice CTA and IVUS were selected. The corresponding coronary lesions were compared between IVUS (20-MHz Eagle-eye; Volcano Inc.) and CTA. A pullback of the IVUS catheter (Volcano Track Back II) was performed automatically at 0.5 mm/s, and the images were stored digitally and assessed offline by a cardiologist. Next, we determined the values for the window width and the level of the corresponding site that exactly equaled the IVUS cross-sectional image in the lumen and vessel sizes. The mean intensity within the lumen at the corresponding sites of 32 coronary plaques was 216 ± 35 HU (mean ± SD), the average window level was 145 ± 23 HU and the average window width was 357 ± 48 HU. In the present study, the average optimal window setting for the lumen and outer vessel boundary was obtained at a level representing 67% ± 2% of the mean intensity within the lumen and a width representing 166% ± 12% of the mean intensity. Therefore, the minimal luminal cross-sectional area (CSA) was measured using a window setting in which the window width was reduced to 1 HU with a window level setting of 67% of the mean intensity within the lumen, whereas the vessel CSA (outer vessel boundary) was determined by a window width of 166% and a window level setting of 67% of the mean intensity within the lumen (Fig. 1). An investigator who had no involvement in any further comparative analyses performed these measurements derived from CTA.

Comparison of 64-Slice CTA and IVUS

Thirty patients were referred for IVUS at the discretion of the referring cardiologist during elective percutaneous coronary intervention on the basis of clinical and imaging findings. The remaining 74 patients underwent no invasive coronary angiography because of normal stress ^{201}Tl or mild reversible defects with mild or intermediate stenosis by CTA. IVUS was performed in 32 coronary plaques of 30 patients using standard techniques after intracoronary injection of 2 mg of isosorbide dinitrate; the results obtained were

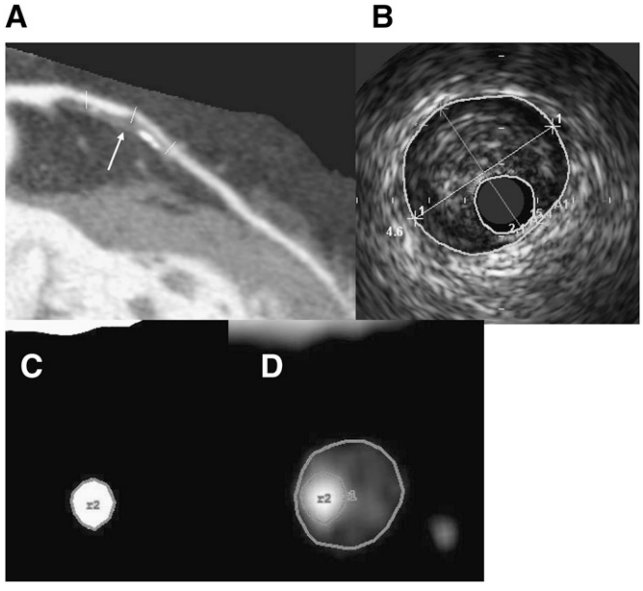

FIGURE 1. Window settings for lumen and outer vessel boundary by CTA are the same as those for IVUS imaging. (A) Curved multiplanar reconstructed CTA image reveals significant stenosis in left anterior descending artery (arrow). (B) IVUS cross-section reveals lumen area of 2.1 mm^2 and vessel area of 15.4 mm^2. Cross-sectional CTA images show luminal CSA of 2.1 mm^2 (C) and vessel CSA of 15.4 mm^2 (D).

compared with the 64-slice CTA-derived data for the same plaques. The lesion lumen and vessel CSAs were determined on cross-sectional images similar to IVUS. The plaque CSA was defined by the difference between the vessel CSA and the lumen CSA. The vessel CSA equaled the external elastic membrane CSA in IVUS, whereas the lumen CSA equaled the internal elastic membrane CSA in IVUS. The lesion percentage stenosis was calculated according to the following formula: plaque CSA/vessel CSA × 100. To ensure that the same corresponding coronary lesions were always compared between IVUS and 64-slice CTA, we determined a landmark such as a side branch for the distal starting reference according to the purpose of the serial IVUS investigation (*14*).

Stress ^{201}Tl SPECT

^{201}Tl SPECT was performed at least 3 d after the CTA. β-Blockers, calcium channel blockers, and nitrates were discontinued for 24–48 h before the test. Furthermore, 78 of the 104 patients underwent symptom-limited exercise on a bicycle ergometer in the sitting position with a 12-lead ECG and blood pressure measurements taken at the baseline and then every minute during the exercise. The test was terminated when the patient achieved 100% of the maximal predicted heart rate, ischemic ST-segment depression of >2 mm, severe cardiac arrhythmia, severe chest pain, or significant hypotension. At the peak of the exercise, a 111-MBq dose of ^{201}Tl was injected intravenously. For 26 patients who were unable to exercise, adenosine was administered intravenously at 0.14 mg/kg/min for 5 min, and ^{201}Tl was injected 3 min into the infusion. The ECG and blood pressure were monitored before and throughout the infusion and again after the infusion. The initial image was obtained at 5 min after the ^{201}Tl injection in the supine position, and a delayed image was obtained 4 h later.

SPECT was performed using a double-detector system (Picker PRISM 2000XP; Shimadzu Corp.) equipped with a low-energy, high-resolution collimator. Seventy-two projection data were obtained with a 64 × 64 matrix over 360°. Data were acquired for 25 s for each projection. The energy window was set at the 67-keV photopeak of ^{201}Tl with a 15% window. Reconstruction was performed using a Butterworth filter at a cutoff frequency of 0.24 cycle per pixel and an order of 8. No attenuation or scatter correction was used. SPECT images were assessed using a 17-segment model, and data were presented in a polar map format (normalized to 100%) (*15*). Perfusion defects were identified on the stress images (segmental tracer activity < 75% of maximum) and divided into ischemia or scar tissue. We used the percentage of peak counts on normalized polar maps within each vascular territory on the stress images as a physiologic measure of quantitative perfusion defects. Stress and delayed images were analyzed independently by 2 nuclear physicians who were unaware of the CTA data. Visual grading was defined as normal (no perfusion defects) or abnormal (stress perfusion defects with redistribution).

Statistical Analysis

All data are expressed as the mean ± SD. Evaluation of statistical differences between groups was performed using the Kruskal–Wallis analysis and Mann–Whitney *U* test. Correlations between measurements determined by CTA and IVUS were estimated using Bland–Altman analysis and Pearson correlation analysis. Mean values were compared using the double-tailed *t* test. One-way ANOVA was used for simultaneous comparison of >2 mean values with a post hoc Turkey–Kramer test. Regression analyses were performed to detect correlations between perfusion data variables and CTA variables. Receiver-operating-characteristic (ROC) analysis was used to determine the optimal cutoff value for detecting functionally significant coronary artery stenosis using stress SPECT. The area under the ROC curve (AUC) provides a measure of the overall accuracy that is independent of the decision criteria, by plotting true-positive rates against false-positive rates as the cutoff level of the model varies. The optimal cutoff value was defined as the point with the highest sum of the sensitivity and specificity. *P* values < 0.05 were considered significant.

RESULTS

Patient Characteristics

The baseline clinical characteristics of the 104 patients are summarized in Table 1. The mean age of the study population was 66.9 ± 11 y, and 76 patients were male (73%). The pretest likelihood of CAD according to Diamond and Forrester (*13*) was low, intermediate, and high in 6 (6%), 78 (75%), and 20 (19%) patients, respectively. The body mass index (BMI) of the patients in the present study was low.

Stress ^{201}Tl Imaging

Among the 104 patients, a reversible defect was observed in 43 patients (41%) (Fig. 2), and normal myocardial perfusion was observed in 61 patients (59%) (Fig. 3). Ten patients (10%) had reversible defects in 2 coronary artery territories. On a vascular territory basis, 259 vascular territories (83%) showed normal myocardial perfusion, and a reversible defect was observed in 53 (17%) vascular territories.

64-Slice CTA Finding

Image quality was excellent in 31 patients (30%), good in 42 patients (40%), adequate in 22 patients (21%), heavily calcified in 6 patients (6%), and with motion artifacts in 3 patients (3%). Nine patients (9%) were nonevaluable: 6 patients with heavy calcification and 3 patients with motion

TABLE 1
Characteristics of Patients (*n* = 104)

Characteristic	Value
Age (y)	66.9 ± 11
Male/female	76/28
Hypertension (%)	55 (53%)
Hyperlipidemia (%)	57 (55%)
Diabetes (%)	41 (39%)
Smoking (%)	47 (45%)
BMI (kg/m^2), median (IQR)	23.8 (21.1–25.6)
Symptoms	
Anginal chest pain	65 (62%)
Atypical chest pain	22 (21%)
Pretest likelihood of CAD	
Low	6 (6%)
Intermediate	78 (75%)
High	20 (19%)
Resting ECG	
Negative T	7 (7%)
ST depression	14 (13%)
Left ventricular hypertrophy	25 (24%)

BMI = body mass index; IQR = interquartile range.

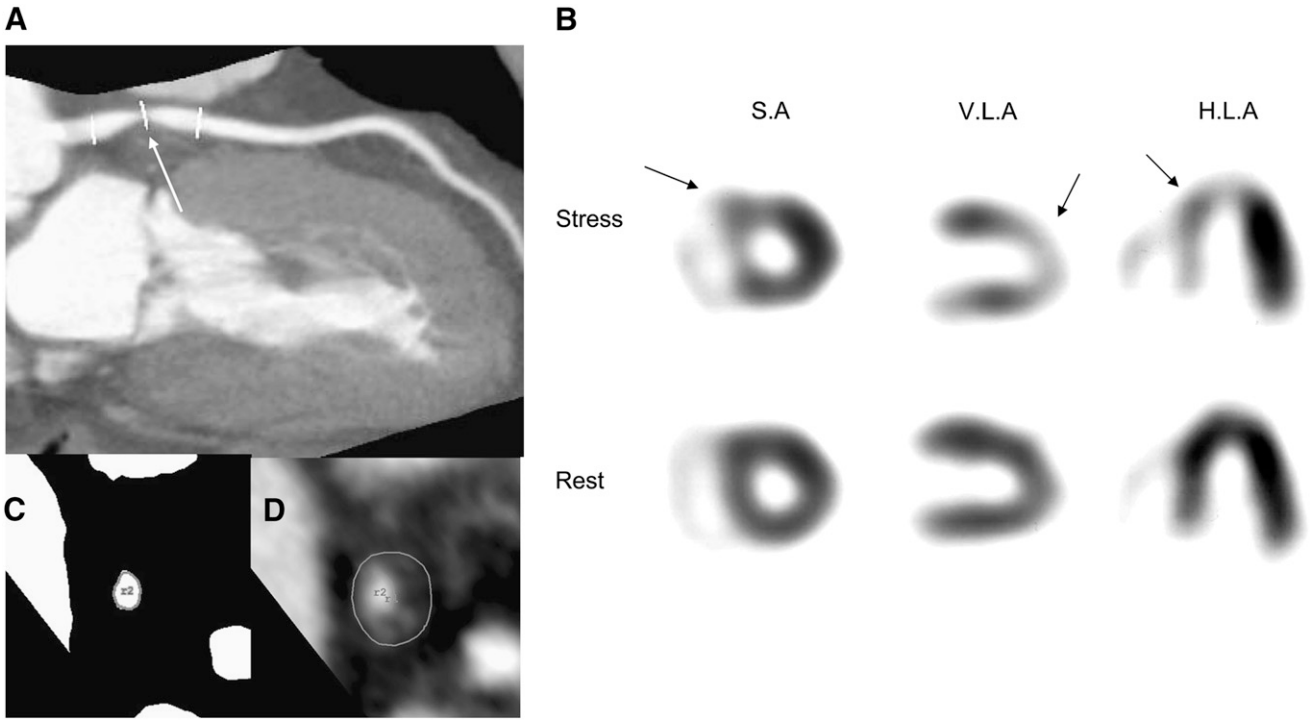

FIGURE 2. A 65-y-old woman with chest pain. (A) CTA image using maximum-intensity projection reveals presence of significant stenosis in proximal left anterior descending artery (arrow). (C) Minimal luminal CSA is 2.6 mm^2. (D) Vessel CSA is 20.9 mm^2. (B) Corresponding tomograms show reversible perfusion abnormality in anterior, septal, and apical wall (arrows). S.A = short axis; V.L.A = vertical long axis; H.L.A = horizontal long axis.

artifacts. On a patient basis, 10 patients (10%) were classified as having a normal coronary artery. Twenty-one patients (20%) showed at least 1 significant stenosis of ≥80%, whereas nonobstructive CAD with stenosis of <60% was observed in 14 patients (13%). Among the remaining 50 patients with intermediate stenosis values of 60%–80%, 16 patients (15%) showed at least 60%–70% stenosis and 34 patients (33%) showed 70%–80% stenosis. On a vessel basis, 180 (63%) of 285 evaluable coronary arteries were normal. CAD was identified in the remaining 105 (37%) coronary arteries, with ≥80% stenosis in 21 (7%), 70%–80% stenosis in 37 (13%), 60%–70% stenosis in 27 (9%), and <60% stenosis in 20 (7%).

Correlations Between CTA Measurements and IVUS Data

We investigated correlations between the stenosis severity by CTA in 32 coronary plaques (12 calcified plaques and 20 noncalcified plaques) of 30 patients and the IVUS data for the same lesions. The mean lesion lumen CSA (3.42 ± 1.0 mm^2 vs. 3.15 ± 1.0 mm^2, $P < 0.01$) and the mean percentage stenosis (74.1% ± 9.5% vs. 74.3% ± 9.3%, $P = 0.85$) were compared between CTA and IVUS, respectively. The correlation coefficients for these measurements were $r = 0.82$ and $r = 0.85$, respectively. A Bland–Altman analysis showed that the lumen CSA measured by CTA was systematically overestimated (mean difference, 0.27 ± 0.64 mm^2), and the percentage stenosis was slightly underestimated (mean difference, −0.22% ± 5.5%) (Fig. 4). For 12 calcified plaques, the correlation coefficients for lumen CSA and percentage stenosis were $r = 0.55$ and $r = 0.73$, respectively. A Bland–Altman analysis showed that the lumen CSA measured by CTA was overestimated (mean difference, 0.60 ± 0.81 mm^2), and the percentage stenosis was slightly underestimated (mean difference, −0.03% ± 5.9%). For 20 noncalcified plaques, the correlation coefficients for these measurements were $r = 0.91$ and $r = 0.87$, respectively. A Bland–Altman analysis showed that the lumen CSA (mean difference, 0.28 ± 0.44 mm^2) and the percentage stenosis (mean difference, 0.14% ± 5.0%) measured by CTA was overestimated (Fig. 4).

The interobserver variability for the minimal luminal CSA measured by CTA was good ($r = 0.87$, $P < 0.001$), and Bland–Altman analysis showed a mean difference of 0.12 ± 0.64 mm^2 between 2 observers ($P = 0.09$). The interobserver variability for the percentage stenosis was good ($r = 0.89$, $P < 0.001$), and Bland–Altman analysis showed a mean difference of −0.87 ± 0.64 mm^2 ($P = 0.09$).

Relationship Between Stenosis Severity by CTA and Perfusion Data

Vessel-Based Analysis. In total, 285 evaluable coronary arteries and related perfusion territories were evaluated. Figure 5 shows the prevalence of reversible defects evaluated by SPECT in the study groups defined according to the percentage stenosis obtained by CTA. In patients with normal

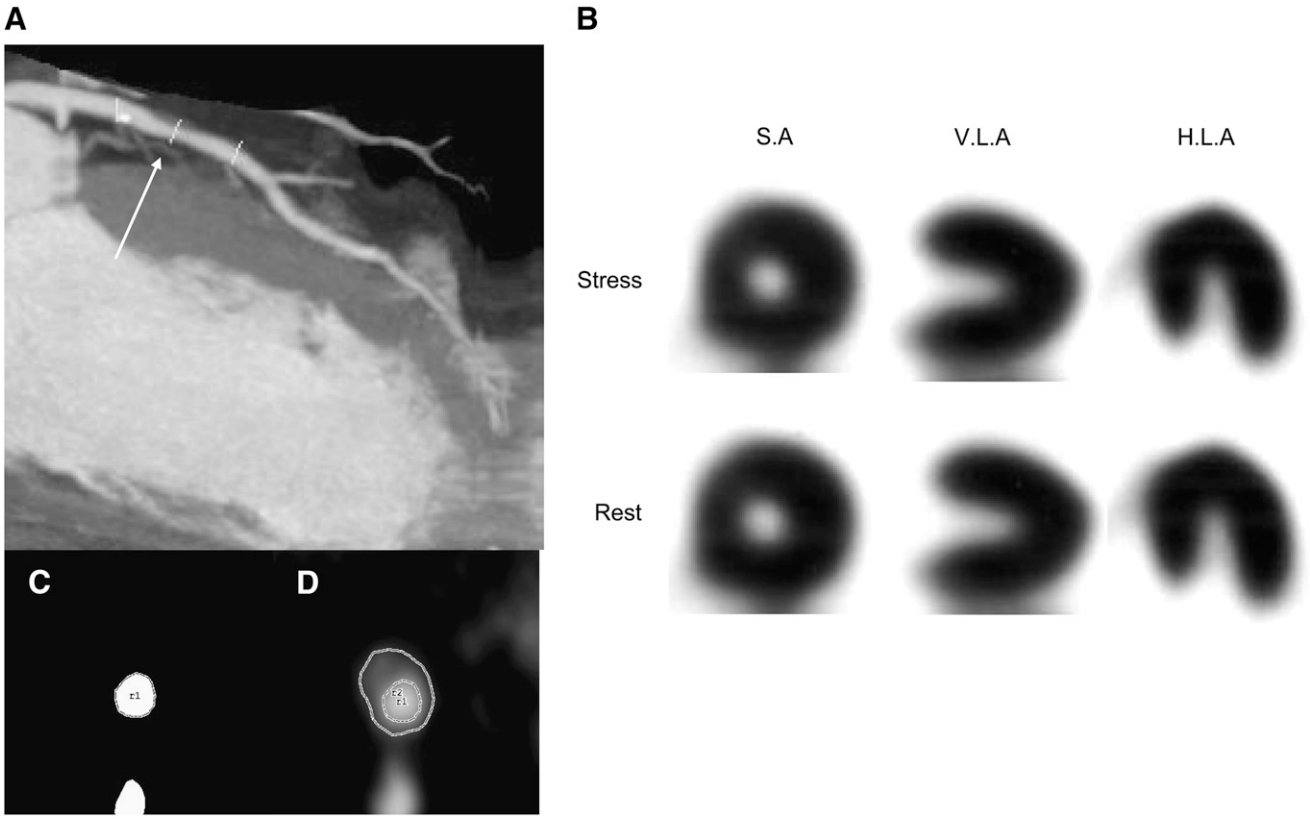

FIGURE 3. A 63-y-old man with chest pain. (A) CTA image using maximum-intensity projection shows noncalcified plaque in left anterior descending artery (arrow). (C) Minimal luminal CSA is 4.2 mm^2. (D) Vessel CSA is 12.5 mm^2. (B) Corresponding tomograms show normal perfusion at peak exercise and rest. S.A = short axis; V.L.A = vertical long axis; H.L.A = horizontal long axis.

coronary arteries, the prevalence of reversible defects was 0%, whereas in patients with 0%–60% stenosis, it was 1 of 20 vessels (5%). Among patients with >60% stenosis, the prevalence of reversible defects significantly increased as the percentage stenosis increased. Among patients with ≥80% stenosis, ischemia was common (86%), whereas for intermediate values of 60%–70% stenosis, the prevalence of reversible defects was 9 of 27 vessels (33%), and for 70%–80% stenosis, the prevalence was 20 of 37 vessels (54%).

Stenosis-Based Analysis. In total, 105 coronary stenoses and related perfusion territories were evaluated. Quantitative stress defects obtained from SPECT significantly increased as the percentage stenosis increased ($r = -0.55, P < 0.0001$) (Fig. 6A). When stenosis was expressed as the minimal luminal CSA by CTA, quantitative stress defects increased significantly as the minimal luminal CSA decreased ($r = 0.52, P < 0.0001$) (Fig. 6B). Quantitative stress defects were lower in the proximal stenosis location than those in the more distal stenosis location (68.9% ± 7.8% vs. 73.5% ± 5.2%, $P = 0.019$).

The SPECT (+) group showed a significantly smaller minimal luminal CSA (2.8 ± 0.6 vs. 4.9 ± 1.4 mm^2, $P < 0.0001$) and more severe percentage area of stenosis (76.6% ± 7.9% vs. 64.1% ± 10.8%, $P < 0.0001$) than that of the SPECT (−) group. However, there were no significant differences in the lesion vessel CSA (13.5 ± 5.8 vs. 14.0 ± 4.2 mm^2, $P = 0.596$) and plaque CSA (10.6 ± 5.5 vs. 9.2 ± 3.7 mm^2, $P = 0.097$) between the 2 groups (Table 2).

Diagnostic Accuracy of Functionally Significant Coronary Artery Stenosis as Determined by CTA Stenosis Thresholds

Table 3 shows the accuracy of CTA measurement of stenosis severity to identify patients with a functional significance of ischemia according to application of stenosis thresholds of >60%, >70%, and >80%. When all nonevaluable vessels were excluded, applying stenosis thresholds of >70% results in 79% sensitivity, 92% specificity, 66% positive predictive value (PPV), and 96% negative predictive value (NPV). When all vessels for analysis with positive nonevaluable vessels were included, applying stenosis thresholds of >70% results in 81% sensitivity, 84% specificity, 51% PPV, and 96% NPV.

ROC Analysis of Functionally Significant Coronary Artery Stenosis Determined by CTA

We performed ROC analyses of the lesion's minimal luminal CSA and the percentage stenosis derived by CTA for detecting functionally significant coronary artery stenosis using stress ^{201}Tl SPECT (Fig. 7). The AUC of the minimal luminal CSA was 0.927, and the best cutoff value was 3.7 mm^2, with a sensitivity of 88% and a specificity of 83%. The AUC of the percentage stenosis was 0.829, and the best cutoff

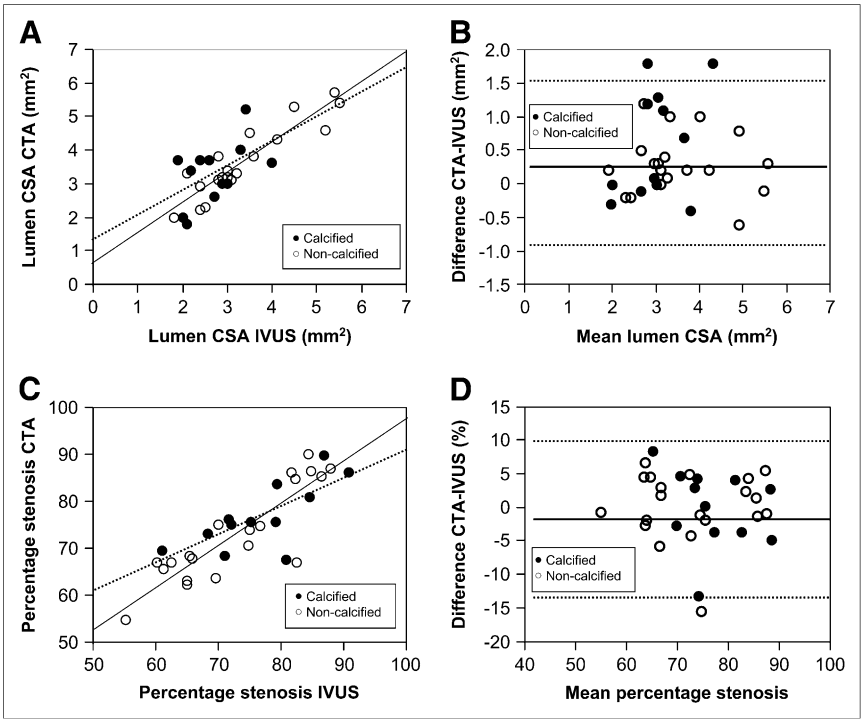

FIGURE 4. (A) Correlation between lumen CSAs measured by 64-slice CTA and IVUS ($n = 32$). Dashed lines correspond to correlation of calcified plaques ($n = 12$, $y = 0.74x + 1.34$, $r = 0.55$, $P = 0.09$), whereas solid lines correspond to correlation of noncalcified plaques ($n = 20$, $y = 0.88x + 0.66$, $r = 0.91$, $P < 0.0001$). (B) Bland–Altman analysis of differences between the lumen CSAs (mean difference, 0.27 ± 0.64 mm^2). Dashed lines correspond to mean $\pm$ 2 SDs (-1.01 to 1.55 mm^2). (C) Correlations between percentage stenosis measured by 64-slice CTA and IVUS ($n = 32$). Dashed lines correspond to correlation of calcified plaques ($n = 12$, $y = 0.61x + 30.1$, $r = 0.73$, $P = 0.0069$), whereas solid lines correspond to correlation of noncalcified plaques ($n = 20$, $y = 0.88x + 8.43$, $r = 0.87$, $P < 0.0001$). (D) Bland–Altman analysis of differences between percentage stenosis (mean difference, $-0.22\% \pm 11\%$). Dashed lines correspond to mean $\pm$ 2 SDs (-11.2% to 10.7%). Open circles indicate noncalcified plaques, whereas solid circles indicate calcified plaques.

value was 71%, with a sensitivity of 75% and a specificity of 76%.

DISCUSSION

The major important findings in the present study are as follows. First, our study demonstrates a relationship between coronary stenosis severity assessed by 64-slice CTA and the severity of defects assessed by stress MPI. Second, despite an excellent NPV to rule out the presence of ischemia, 64-slice CTA provides limited accuracy for identifying the physiologic significance of inducible perfusion defects in this highly selected patient group. In the range between 60% and 80% stenosis, there is a substantial scatter in the correlation of function (^{201}Tl scintigraphy) and morphology. Therefore, on an individual level, there is a need for an additional functional procedure such as a perfusion measurement.

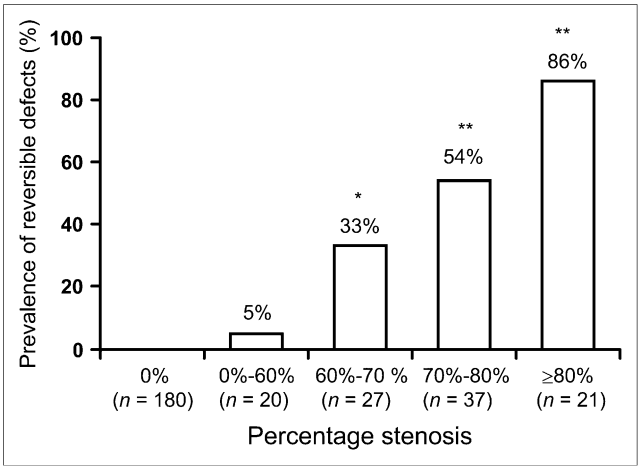

FIGURE 5. Prevalence of reversible defects evaluated by SPECT in study groups defined according to percentage stenosis obtained by CTA. Numbers under the bars represent number of vessels. *$P = 0.018$. **$P < 0.0001$ vs. percentage stenosis of 0%–60%.

Comparison Between CTA and IVUS

The recent introduction of CTA scanners with submillimeter slice collimation has increased the spatial and temporal resolution and improved our ability to measure the dimensions of coronary plaques and vessels (*12,16,17*). In the present study, the lumen CSA and the percentage stenosis of 32 de novo coronary lesions measured by CTA were closely correlated with those obtained by IVUS; however, the lumen CSA measured by CTA was overestimated and the percentage stenosis was slightly underestimated. Although we presented the correlations with IVUS separately for calcified and noncalcified plaques, there are some limitations to accurately quantify the calcified plaques due to the partial-volume effects. Leber et al. demonstrated that 64-slice CTA-derived measurements showed good correlations with IVUS for lumen and plaque area determinations using individually adapted window settings; however, their ability to quantify the grade of a luminal obstruction was limited by the significant trend toward overestimation of the lumen area and underestimation of the plaque area (*12*).

Previous landmark studies by Achenbach and colleagues reported rather poor correlations between noncalcified plaques assessed by quantitative 16-slice CTA and IVUS (*17,18*). This is also relevant because patients with severe

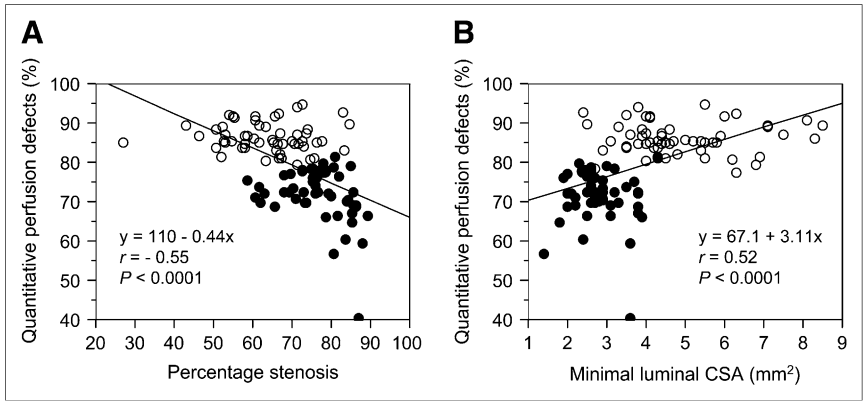

FIGURE 6. (A) Quantitative perfusion defects in relation to percentage stenosis by CTA. (B) Quantitative perfusion defects in relation to minimal luminal CSA. Open circles indicate negative SPECT, and solid circles indicate positive SPECT.

calcification were excluded from the current study. However, it is most likely that the improved spatial resolution of the scanner with thinner detectors (0.5 mm) used in the current study increased the sensitivity of the detection of noncalcified lesions. Another factor may be the low BMI in our study population, as elevated BMI leads to a poor signal-to-noise ratio, which in turn is a limiting factor in cardiac scanning. Raff et al. demonstrated that when BMI was normal (<25 kg/m^2), sensitivity, specificity, PPV, and NPV were all 100% (*11*). A previous study that used 64-slice CTA also increased the detection sensitivity for noncalcified lesions to 83% (*19*). A BMI of <25 kg/m^2 on average in the patient group is very uncommon in the United States and in Europe. The previously proposed cutoff values for cardiovascular risk factors cannot be applied to nonwestern populations because the average BMI and waist circumference for Asians are smaller (*20*). Several studies in Asia report that for the definition of obesity in Asians, the cutoff value for BMI is 23 kg/m^2 and for waist circumference it is 90 cm for men and 80 cm for women (*21*). A 10-y cohort study of national heath insurance in a Japanese population showed that the excess medical expenditures by risk clustering of normal weight categories within the total medical expenditures were higher than those of overweight categories because more participants were of normal weight (*22*). Therefore, in the present study, there was no potential selection bias that influences the body habitus.

Relationship Between Stenosis Severity by CTA and Perfusion Data

To our knowledge, no previous studies have demonstrated a relationship between the severity of stenosis revealed by CTA and the severity of defects revealed by stress MPI. We found that reversible defects began to increase progressively when the area of stenosis was at least 60%. This observation is consistent with the findings that basal myocardial blood flow remains constant regardless of the severity of coronary artery stenosis, and the maximal flow starts to diminish progressively when the luminal diameter stenosis is about 40% or more—which is equivalent to 60% if the stenosis is expressed in terms of the area of stenosis—and does not differ significantly from the basal flow when the luminal diameter stenosis diameter is ≥80% (*23*). In the present study, ischemia is common for a stenosis severity of ≥80% by CTA and is seldom observed for a value of <60%. For intermediate values of 60%–70% stenosis, the prevalence of reversible defects was 9 of 27 vessels (33%), and for 70%–80% stenosis the prevalence was 20 of 37 vessels (54%). Schuijf et al. showed that only 39% of obstructed vessels (≥50% luminal narrowing) have abnormal MPI (*24*), and lesions with an intermediate severity of stenosis vary in hemodynamic significance (*25*). The present study demonstrated that the NPV of CTA to exclude the presence of ischemia is excellent, but its PPV or ability to identify

TABLE 2
Comparison of 64-Slice CTA Measurements According to Stress ^{201}Tl SPECT Results

	Lesion			
SPECT result	Minimal luminal CSA (mm^2)	Vessel CSA (mm^2)	Plaque CSA (mm^2)	Stenosis (%)
(+) (n = 48)	2.8 ± 0.6*	13.5 ± 5.8	10.6 ± 5.5	76.6 ± 7.9*
(−) (n = 57)	4.9 ± 1.4	14.0 ± 4.2	9.2 ± 3.7	64.1 ± 10.8

*P < 0.0001 vs. SPECT (−).

TABLE 3
Diagnostic Accuracy of Functionally Significant Coronary Artery Stenosis According to Stenosis Severity by 64-Slice CTA

Stenosis criterion (%)	Sensitivity (%)	Specificity (%)	PPV (%)	NPV (%)
Vessels for analysis only with evaluable vessels				
>60	98	84	55	99
>70	79	92	66	96
>80	38	98	86	89
All vessels for analysis with positive nonevaluable vessels				
>60	98	77	46	99
>70	81	84	51	96
>80	43	90	48	89

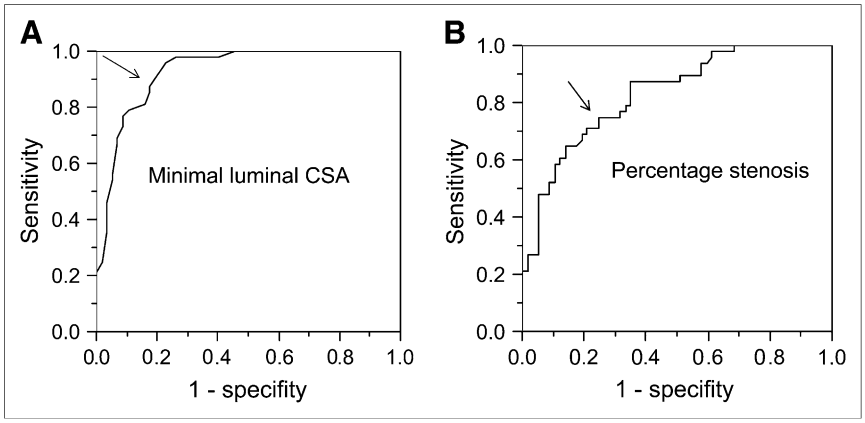

FIGURE 7. Diagnostic value of CTA measurements for assessment of functionally significant coronary artery stenosis using stress ^{201}Tl SPECT. ROC curves of lesion luminal CSA (A) and lesion percentage stenosis (B).

patients with ischemia is rather poor. This finding is consistent with what has been reported (*26*).

The present study found that the lesion minimal luminal CSA (cutoff value of 3.7 mm^2) measured by 64-slice CTA shows good diagnostic values of 88% sensitivity and 83% specificity for identifying physiologically significant coronary stenosis associated with stress MPI. A previous report documented a high diagnostic accuracy—for an IVUS luminal area of 4.0 mm^2 at the lesion site—for predicting significant coronary narrowing using stress MPI (*7*). Abizaid et al. demonstrated a high diagnostic accuracy—for a lesion minimal luminal area of 4.0 mm^2 determined by IVUS—for predicting an abnormal coronary flow reserve of 2.0 revealed by intracoronary Doppler flow (*27*). This finding is consistent with our results, in which a slightly lower cutoff value of 3.7 mm^2 was chosen to optimize the discrimination between normal and abnormal perfusion in our population. In the present study, our ROC analysis further supported the usefulness of the percentage stenosis of the lesion for identifying the physiologic significance of perfusion defects, with 75% sensitivity and 76% specificity. The minimal luminal area of the lesion derived by CTA is simpler and superior to the percentage area of stenosis of the lesion for identifying inducible perfusion defects. However, the use of 64-slice CTA in a broader clinical application—to the individual body habitus of the patient (normalization) or the adjacent normal vessel structures—requires adjustment of the cutoff value for probably significant stenosis. Theoretically, it can be hypothesized that a small luminal area does not necessarily cause ischemia in small vessels. Therefore, small vessels were excluded from the present study, and the luminal area of the lesion can be validated to detect significant coronary stenosis in the proximal and middle segments. There were no differences in the vessel and plaque areas between the SPECT (+) and SPECT (−) groups. This result could be explained by the fact that our study population excluded patients with unstable angina. Previous studies have demonstrated that lesions in vessels with positive remodeling are highly associated with high lipid contents and macrophage counts in patients with unstable angina, whereas negative remodeling tends to be associated with high-grade luminal stenosis in patients with stable angina (*28,29*).

Finally, the advantage of CTA as compared with invasive functional measurements—such as IVUS, intracoronary Doppler flow, and transstenotic pressure measurements—is its noninvasive character. Furthermore, CTA contributes important morphologic information in addition to evaluating the functional significance of coronary stenosis with stress MPI.

Clinical Limitations

First, we used standard 4-h delay images without thallium reinjection, which could result in underestimation of the extent and severity of myocardial ischemia, especially in patients with a prior infarction. Furthermore, there were some technical limitations associated with thallium imaging, such as breast, diaphragmatic, and soft-tissue attenuation. Attenuation artifacts for ^{99m}Tc-labeled myocardial perfusion agents will be somewhat less marked than those for ^{201}Tl (*30*). A gated SPECT study with a ^{99m}Tc-labeled perfusion maker with an automated image analysis package is more appropriate (*31,32*). Ideally, the minimal luminal diameter measurements would be correlated with a quantitative method such as PET. Further investigations using these modalities are required to prospectively test the predictive accuracy of our proposed quantitative cutoff values for identifying ischemia.

Second, the sample size was small and the study population was limited to selected patients chosen for excellent CTA image quality with the absence of motion artifacts or severe calcification. Furthermore, the study subjects were predominantly male, presumably with larger coronary arteries, and the patient population had very low BMIs as compared with typical coronary heart disease patients in the United State or Europe. Patients with serial stenosis or microvascular disease also were excluded from the patient population. The proposed threshold value for CSA is valid in this highly selected patient group. For example, women would probably have a different threshold value. Thus, we acknowledge that our patient population was an idealized

dataset, and whether the results can be generalized to broader populations—including those with smaller vessels, more calcified vessels, and so forth—awaits further validation.

CONCLUSION

A comparison of 64-slice CTA measurements and stress MPI revealed that despite an excellent NPV to rule out the presence of ischemia, 64-slice CTA alone is a poor discriminator of the functional significance of myocardial ischemia in a highly selected patient population with a low BMI. It is clinically relevant that both CTA and stress MPI provide complementary information—namely, anatomic data and physiologic data—in evaluating coronary lesions with intermediate stenosis severity to prevent an unnecessarily high number of revascularization procedures.

REFERENCES

1. White C, Wright C, Doty DB, et al. Does visual interpretation of the coronary arteriogram predict the physiologic importance of a coronary stenosis? *N Engl J Med.* 1984;310:819–824.
2. Marcus ML, Harrison DG, White CW, McPherson DD, Wilson RF, Kerber RE. Assessing the physiologic significance of coronary obstructions in patients: importance of diffuse undetected atherosclerosis. *Prog Cardiovasc Dis.* 1988;31:39–56.
3. Vogel RA. Assessing stenosis significance by coronary arteriography: Are the best variables good enough? *J Am Coll Cardiol.* 1988;12:692–693.
4. Machecourt J, Longere P, Fagret D, et al. Prognostic value of thallium-201 single-photon emission computed tomographic myocardial perfusion imaging according to extent of myocardial defect: study in 1926 patients with follow-up at 33 months. *J Am Coll Cardiol.* 1994;23:1096–1106.
5. Brown KA, Altland E, Rowen M. Prognostic value of normal technetium-99m sestamibi cardiac imaging. *J Nucl Med.* 1994;35:554–557.
6. Iskander S, Iskandrain AE. Risk assessment using single-photon emission computed tomographic technetium-99m sestamibi imaging. *J Am Coll Cardiol.* 1998;32:57–62.
7. Nishioka T, Amanullah AM, Luo H, et al. Clinical validation of intravascular ultrasound imaging for assessment of coronary stenosis severity: comparison with stress myocardial perfusion imaging. *J Am Coll Cardiol.* 1999;33:1870–1878.
8. Pijls NHJ, Bruyne B, Peels K, et al. Measurement of fractional flow reserve to assess the functional severity of coronary artery stenosis. *N Engl J Med.* 1996;334:1703–1708.
9. Ropers D, Baum U, Pohle K, et al. Detection of coronary artery stenoses with thin-slice multi-detector row spiral computed tomography and multiplanar reconstruction. *Circulation.* 2003;107:664–666.
10. Achenbach S, Ropers D, Hoffmann U, et al. Assessment of coronary remodeling in stenotic and nonstenotic coronary atherosclerotic lesions by multidetector spiral computed tomography. *J Am Coll Cardiol.* 2004;43:842–847.
11. Raff GL, Gallagher MJ, O'Neill WW, Goldstein JA. Diagnostic accuracy of noninvasive coronary angiography using 64-slice spiral computed tomography. *J Am Coll Cardiol.* 2005;46:552–557.
12. Leber AW, Knez A, von Ziegler F, et al. Quantification of obstructive and nonobstructive coronary lesions by 64-slice computed tomography: a comparative study with quantitative coronary angiography and intravascular ultrasound. *J Am Coll Cardiol.* 2005;46:147–154.
13. Diamond GA, Forrester JS. Analysis of probability as an aid in the clinical diagnosis of coronary artery disease. *N Engl J Med.* 1979;300:1350–1358.
14. Mintz GS, Nissen SE, Anderson WD, et al. American College of Cardiology Clinical Expert Consensus Document on Standards for Acquisition, Measurement and Reporting of Intravascular Ultrasound Studies (IVUS): a report of the American College of Cardiology Task Force on Clinical Expert Consensus Documents. *J Am Coll Cardiol.* 2001;37:1478–1492.
15. Cerqueira MD, Weissman NJ, Dilsizian V, et al. Standardized myocardial segmentation and nomenclature for tomographic imaging of the heart: a statement for healthcare professionals from the Cardiac Imaging Committee of the Council on Clinical Cardiology of the American Heart Association. *Circulation.* 2002;105:539–542.
16. Mollet NR, Cademartiri F, van Mieghem CAG, et al. High-resolution spiral computed tomography coronary angiography in patients referred for diagnostic conventional coronary angiography. *Circulation.* 2005;112:2318–2323.
17. Leber AW, Knez A, Becker A, et al. Accuracy of multidetector spiral computed tomography in identifying and differentiating the composition of coronary atherosclerotic plaques: a comparative study with intracoronary ultrasound. *J Am Coll Cardiol.* 2004;43:1241–1247.
18. Achenbach S, Moselewski F, Ropers D, et al. Detection of calcified and noncalcified coronary atherosclerotic plaque by contrast-enhanced, submillimeter multidetector spiral computed tomography: a segment-based comparison with intravascular ultrasound. *Circulation.* 2004;109:14–17.
19. Leber AW, Becker A, Knez A, et al. Accuracy of 64-slice computed tomography to classify and quantify plaque volumes in the proximal coronary system: a comparative study using intravascular ultrasound. *J Am Coll Cardiol.* 2006;47:672–677.
20. Tan CE, Ma S, Wai D, Chew SK, Tai ES. Can we apply the National Cholesterol Education Program Adult Treatment Panel definition of the metabolic syndrome to Asians? *Diabetes Care.* 2004;27:1182–1186.
21. Snehalatha C, Viswanathan V, Ramachandran A. Cutoff values for normal anthropometric variables in Asian Indian adults. *Diabetes Care.* 2003;26:1380–1384.
22. Okamura T, Nakamura K, Kanda H, et al. Effect of combined cardiovascular risk factors on individual and population medical expenditures: a 10-year cohort study of national heath insurance in a Japanese population. *Circ J.* 2007;71:807–813.
23. Uren NG, Melin JA, Bruyne BD, Wijns W, Baudhuin T, Camici PG. Relation between myocardial blood flow and the severity of coronary artery stenosis. *N Engl J Med.* 1994;330:1782–1788.
24. Schuijf JD, Wijns W, Jukema JW, et al. Relationship between noninvasive coronary angiography with multi-slice computed tomography and myocardial perfusion imaging. *J Am Coll Cardiol.* 2006;48:2508–2514.
25. Heller LI, Cates C, Popma J, et al. Intracoronary Doppler assessment of moderate coronary artery disease: comparison with ^{201}Tl imaging and coronary angiography: FACTS Study Group. *Circulation.* 1997;96:484–490.
26. Hacker M, Jakob T, Matthiesen F, et al. Comparison of spiral multidetector CT angiography and myocardial perfusion imaging in the noninvasive detection of functionally relevant coronary artery lesions: first clinical experiences. *J Nucl Med.* 2005;46:1294–1300.
27. Abizaid A, Mintz GS, Pichard AD, et al. Clinical, intravascular ultrasound, and quantitative angiographic determinants of the coronary flow reserve before and after percutaneous transluminal coronary angioplasty. *Am J Cardiol.* 1998;82:423–428.
28. Schoenhagen P, Ziada KM, Kapadia SR, Crowe TD, Nissen SE, Tuzcu M. Extent and direction of arterial remodeling in stable versus unstable coronary syndromes: an intravascular ultrasound study. *Circulation.* 2000;101:598–603.
29. Pasterkamp G, Schoneveld AH, van der Wal AC, et al. Relation of arterial geometry to luminal narrowing and histologic makers for plaque vulnerability: the remodeling paradox. *J Am Coll Cardiol.* 1998;32:655–662.
30. Manglos SH, Thomas FD, Gagne GM, Hellwig BJ. Phantom study of breast tissue attenuation in myocardial imaging. *J Nucl Med.* 1993;34:992–996.
31. Smanio PE, Watson DD, Segalla DL, et al. Value of gating of ^{99m}Tc-sestamibi single-photon emission computed tomographic imaging. *J Am Coll Cardiol.* 1997;30:1687–1692.
32. Hendel RC, Corbett JR, Cullom SJ, et al. The value and practice of attenuation correction for myocardial perfusion SPECT imaging: a joint position statement from the American Society of Nuclear Cardiology and the Society of Nuclear Medicine. *J Nucl Cardiol.* 2002;9:135–143.